# Towards a Pixel TPC: construction and test of a 32 chip GridPix detector

M. van Beuzekom[a], Y. Bilevych[b], K. Desch[b], S. van Doesburg[a], H. van der Graaf[a], J. Kaminski[b], P.M. Kluit[a], N. van der Kolk[a], C. Ligtenberg[a], G. Raven[a], J. Timmermans[a]

[a]*Nikhef, Science Park 105, 1098 XG Amsterdam, The Netherlands*
[b]*Physikalisches Institut, University of Bonn, Nussallee 12, 53115 Bonn, Germany*

**Abstract**

A Time Projection Chamber (TPC) module with 32 GridPix chips was constructed and the performance was measured using data taken in a test beam at DESY in 2021. The GridPix chips each consist of a Timepix3 chip with integrated amplification grid and have a high efficiency to detect single ionisation electrons. In the test beam setup, the module was placed in between two sets of Mimosa silicon detector planes that provided external high precision tracking and the whole detector setup was slided into the PCMAG magnet at DESY. The analysed data were taken at electron beam energies of 5 and 6 GeV and at magnetic fields of 0 and 1 Tesla(T).

The result for the transverse diffusion coefficient $D_T$ is 287 µm/$\sqrt{cm}$ at B = 0 T and $D_T$ is 120 µm/$\sqrt{cm}$ at B = 1 T. The longitudinal diffusion coefficient $D_L$ is measured to be 268 µm/$\sqrt{cm}$ at B = 0 T and 250 µm/$\sqrt{cm}$ at B = 1 T. Results for the tracking systematical uncertainties in xy (pixel plane) were measured to be smaller than 14 µm with and without magnetic field. The tracking systematical uncertainties in z (drift direction) were smaller than 14 µm (B = 0 T) and 22 µm (B = 1 T). Finally, the result for the $dE/dx$ resolution for a MIP particle based on a 1 meter track and a realistic GridPix coverage of 60% was measured to be 4% in a 1 T magnetic field.

*Keywords:* Micromegas, gaseous pixel detector, micro-pattern gaseous

*Corresponding author. Telephone: +31 20 592 2000
*Email address:* s01@nikhef.nl (P.M. Kluit)

detector, Timepix, GridPix, pixel time projection chamber

---

## 1. Introduction

Earlier publications on a single chip [1] and four chip (quad) GridPix detectors [2] showed the potential of the GridPix technology and the large range of applications for these devices [3]. In particular, it was demonstrated that single ionisation electrons can be detected with high efficiency and great precision, allowing an excellent track 3D position measurements and particle identification based on the number of electrons and clusters.

As a next step towards a Pixel Time Projection Chamber for a future collider experiment [4], [5], a module consisting of 32 GridPix chips based on the Timepix3 chip was constructed.

A GridPix detector consists of a CMOS pixel Timepix3 chip [6] with integrated amplification grid added by Micro-electromechanical Systems (MEMS) postprocessing techniques. The Timepix3 chip can be operated with a low threshold of 515 $e^-$, and has a low equivalent noise charge of about 70 $e^-$. The GridPix single chip and quad detectors have a very fine granularity of $55\,\mu m \times 55\,\mu m$ and a high efficiency to detect single ionisation electrons.

Based on the experience gained with these detectors a 32 GrixPix chip module - consisting of 8 quads - was built. A drift box defining the electric field and gas envelop was constructed. A readout system for up to 128 chips with 4 multiplexers readout by one speedy pixel detector readout SPIDR board [7] [8] was designed. After a series of tests using the laser setup and cosmics in the laboratory at Nikhef [9], the detector was taken to DESY for a two week test beam campaign.

At DESY the 32 chip detector was placed in between two sets of Mimosa silicon detector planes and mounted on a movable stage. The whole detector setup was slided into the centre of the PCMAG magnet at DESY. A beam trigger was provided by scintillator counters. The data reported here were taken at different stage positions and electron beam momenta of 5 and 6 $GeV/c$ and at magnetic fields of 0 and 1 Tesla(T). The performance of the 32 GrixPix chip module was measured using these data sets.

## 2. 32 GridPix chip module

A 32 GrixPix chip module was built using the quad module [2] as a basic building block. The quad module consists of four GridPix chips and is optimised for a high fraction of sensitive area of 68.9%. The external dimensions are 39.6 mm × 28.38 mm. The four chips which are mounted on a cooled base plate (COCA), are connected with wire bonds to a common central 6 mm wide PCB. A 10 mm wide guard electrode is placed over the wire bonds 1.1 mm above the aluminium grids, in order to prevent field distortions of the electric drift field. The guard is the main inactive area, and its dimensions are set by the space required for the wire bonds. On the back side of the quad module, the PCB is connected to a low voltage regulator. The aluminium grids of the GridPixes are connected by 80 µm insulated copper wires to a high voltage (HV) filtering board. The quad module consumes about 8 W of power of which 2 W is used in the LV regulator.

Eight quad modules were embedded in a box, resulting in a GridPix module with a total of 32 chips. A schematic 3-dimensional drawing of the detector is shown in Figure 1. A schematic drawing of the quads in the module is shown in Figure 2, where also the beam direction is indicated.

The internal dimensions of the box are 79 mm along the $x$-axis, 192 mm along the $y$-axis, and 53 mm along the $z$-axis (drift direction), and it has a maximum drift length (distance between cathode and readout anode) of 40 mm. The drift field is shaped by a series of parallel CuBe field wires of 50 µm diameter with a wire pitch of 2 mm and guard strips are located on all of the four sides of the active area. In addition, six guard wires - shown with dashed lines in Figure 2 - are suspended over the boundaries of the chips, where no guard is present, to minimize distortions of the electric drift field. The wires are located at a distance of 1.15 mm from the grid planes, and their potential is set to the potential at

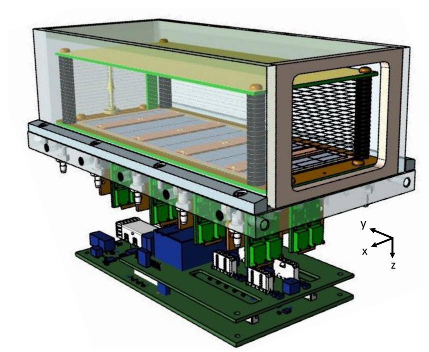


Figure 1: Schematic 3-dimensional render of the 8-quad module detector for illustration purposes.

this drift distance. The box has two Kapton 50 µm windows to allow the beam to pass with minimal multiple scattering.

The data acquisition system of the quad module was adopted to allow for multiple quads to be readout. A multiplexer card was developed that handles four quads or 16 chips and combines the Timepix3 data into one data stream. For the 32 GrixPix module two multiplexers are connected to a SPIDR board that controls the chips and readout process. The readout speed per chip is 160 Mbps and for the multiplexer 2.56 Gbps this corresponds to a maximum

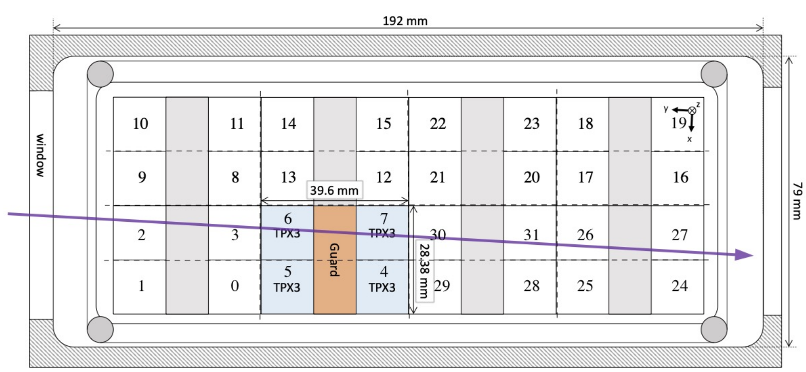


Figure 2: Schematic drawing of the 8-quad module detector with one example quad. The chips are numbered and the beam direction is shown in purple.

rate of 21 MHits/s. For each pixel the precise Time of Arrival (ToA) using a 640 MHz TDC and the time over threshold (ToT) are measured.

The gas volume of 780 ml is continuously flushed at a rate of ∼50 ml/min with premixed T2K TPC gas. This gas is a mixture consisting of 95 % Ar, 3 % $CF_4$, and 2 % $iC_4H_{10}$ suitable for large TPCs because of the relatively high drift velocity and the low diffusion in a magnetic field.

## 3. Experimental setup

In preparation of the two weeks DESY test beam campaign, a support frame was designed to move the 32 chip GridPix module in the transverse plane perpendicular to the beam by a remotely controlled stage such that the whole detector volume could be probed. The support frame also held three Mimosa 26 silicon detector planes [10] placed in front of the detector and three Mimosa planes behind the detector. At DESY the Mimosa silicon detector planes that were provided by the test beam coordinators were mounted. The whole detector setup was slided into the centre of the PCMAG magnet at the DESY test beam facility II [10]. A beam trigger was provided by scintillator counters. The data were taken at different stage positions to cover the whole sensitive TPC volume. Runs with electron beam momenta of 5 and 6 $GeV/c$ and at magnetic fields of 0 and 1 Tesla(T) were analysed.

A photograph of the detector setup in the PCMAG magnet is shown in Figure 3.

The experimental and environmental parameters such as temperature, pressure, gas flow, oxyxgen content were measured and logged by a Windows operated slow control system. The experimental parameters are summarised in Table 1. The chips were cooled by circulating Glycol through the cooling channels in the module carrier plate. The cooling blocks of the concentrators were further cooled by blowing pressurised air on them.

The data was produced in four main data streams: one stream produced by the Mimosa Telescope, two data streams by the two Timepix concentrators and

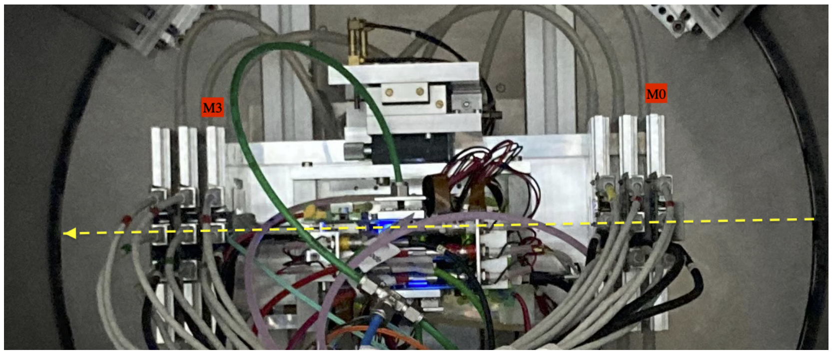


Figure 3: Photo of the detector setup at the centre of the PCMAG magnet. The Mimosa planes M0 and M3 are indidated in red as well as the beam direction (yellow). Centrally, the stager positions the TPC module such that the beam passes through.

Table 1: Overview of the experimental parameters. The ranges indicate the variation over the data taking period

| | |
|---|---|
| Number of analysed runs at B=0 (1) Tesla | 6 (8) |
| Run duration | 10-90 minutes |
| Number of triggers | 3-100 k |
| $E_{\text{drift}}$ | 280 V/cm |
| $V_{\text{grid}}$ | 340 V |
| Threshold | 550 $e^-$ |
| Gas Temperature | 303.3-306.6 K |
| Pressure | 1011 – 1023 mbar |
| Oxygen concentration | 240 - 620 ppm |
| Water vapour concentration | 2000 - 7000 ppm |

one trigger stream. A scintillator provided a trigger signal to the Trigger Logic Unit (TLU) [11] that sends a signal to the trigger SPIDR and telescope readout. The data acquisition system of the Telescope and trigger SPIDR injected a timestamp into their respective data streams. Hits from the Mimosa planes were collected with a sliding window of $-115$ ms to $230$ ms of the trigger. The data acquisition of the concentrator and the trigger SPIDR were synchronized at the start of the run. By comparing the time stamps in these streams, Telescope tracks and TPC tracks could be matched. Unfortunately, the SPIDR trigger had - due to a cabling mistake at the output of the TLU - a common 25 nsec jitter.

In the first week of the test beam period it was found out that three HV cables had a bad connection. The cables were replaced and the module could be fully operated. Unfortunately, after a short data taking period one of the chips (nr 11) developed a short circuit and the HV on the grid of the chip was disconnected. Only after the test beam data taking period the module was repaired in the clean room in Bonn.

## 4. Analysis

### *4.1. Telescope Track reconstruction procedure*

The data of the Telescope is decoded and analysed using the Corryvreckan software package [12]. The track model used for fitting was the general broken lines (GBL) software [13]. The code was extended and optmized to fit curved broken lines for the data with a magnetic field. The telescope planes were iteratively aligned using the standard alignment software provided by the package. The single point Mimosa resolution is 4 µm in x and 6 µm in z (drift direction).

Telesope tracks were selected with at least 5 out of the 6 plane on the track and a total $\chi^2$ of better than 25 per degree of freedom. The uncertainties on the Telescope track prediction in the middle of the GridPix module are dominated by multiple scattering. For a 6 $GeV/c$ track with no magnetic field they can be measured comparing the predictions from the two telescope arms. The expected uncertainty in x and z is 26 µm on average.

### 4.2. TPC Track reconstruction procedure

GridPx hits are selected requiring a minimum time over threshold ToT of 0.15 µs. The drift time is defined as the measured time of arrival minus the trigger time recorded in the trigger SPIDR data stream. The drift time was corrected for time slewing [2] using the measured time over threshold (ToT) and the formula 1:

$$\delta t = \frac{18.6(ns)}{\mathrm{ToT} + 0.1577(\mu s)}. \tag{1}$$

Furthermore, small time shifts corrections - with an odd-even and a $16 \times 2$ pixels structure - coming from the TPX3 clock distribution were extracted from the data and applied.

The $z$-coordinate - i.e. the drift length - was calculated from the drift time and the drift velocity. GridPix hits outside a Telescope acceptance window in x ($\pm$ 15 mm) and z ($\pm$ 7.5 mm) were not used in the track finding and reconstruction. Based on a Hough transform an estimate of the TPC track position and angles in the middle of the module (at y = 1436 pixels) was obtained. This estimate was used to collect the hits around the TPC track and fit the track parameters. For this fit a straight line (B=0 Tesla) or a quadratic track (B=1 Tesla) model was used. In the fit, the expected uncertainties per hit $\sigma_x$ and $\sigma_z$ were used. The fit was iterated three times to perform outlier removal at respectively 10, 5 and 2.5 sigma level. A TPC track was required to have a least 100 hits in each concentrator. At least 25% of the total number of hits should be on track and the $\chi^2$ per degree of freedom has to be less than 3 in xy and z. All track parameters were expressed at a plane the middle of the TPC.

The drift velocity was calibrated per run comparing the Telescope tracks to the TPC hits. For the B=0 field runs it varies between 0.0616 and 0.0630 mm/ns. For the B=1 Tesla runs between 0.0572 and 0.0591 mm/ns. The variation comes mainly from the changes in the relative humidity of the gas volume due to small

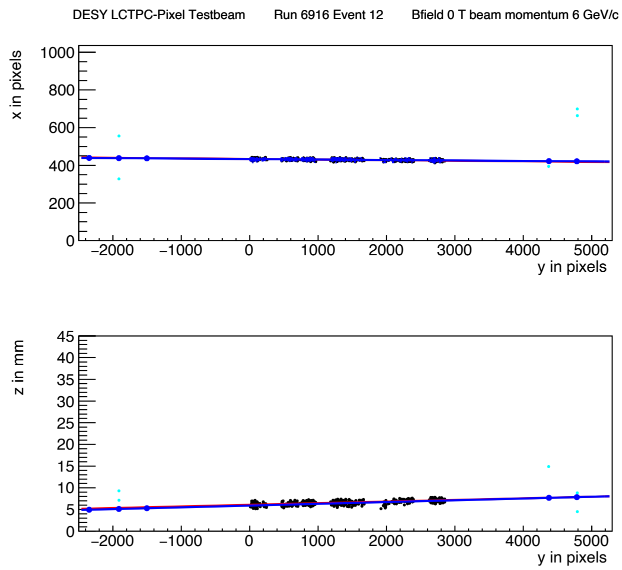


Figure 4: An event display for run 6913 without B field, with 1293 TPC hits (black dots) in the precision plane (xy) and driftplane (zy). The fitted TPC track (red line) with 1130 hits on is and the telescope track (blue line) with 5 Mimosa planes (blue hits) on track are shown. In green the off track Mimosa hits are shown.

leaks. The individual TPX3 chips were aligned fitting a shift in x (z) and two slopes dx(z)/d row(column). The alignment was done per run, because the detector was moved in and x and or z for each run. The fitted slopes also corrected for small shifts and rotations (3D) in the nominal chip position.

An example event run 6913 without B field with a TPC and a telescope track is shown in figure 4. The TPC is located between y = 0 and 2872 pixels. Three Mimosa planes are located at y ¡ -1000 and three at y ¿ 4000 pixels.

### *4.3. Track selections*

In order to study the single electron resolution for the data with and without magnetic field, additional selections on the Telescope and TPC tracks were applied to select high quality tracks. Due to the trigger time jitter of 25 nsec, the prediction of the telescope track in z must be used as the reference for z. Secondly, the z hits of the TPC track were fitted to correct for the common

Table 2: Table with track selection cuts

| Event Selection |
|---|
| $\lvert x_{\text{TPC}} - x_{\text{Telescope}}\rvert < 0.3\,\text{mm}$ |
| $\lvert z_{\text{TPC}} - z_{\text{Telescope}}\rvert < 2.0\,\text{mm}$ |
| $\lvert dx/dy_{\text{TPC}} - dx/dy_{\text{Telescope}}\rvert < 4\,\text{mrad}$ |
| $\lvert dz/dy_{\text{TPC}} - dz/dy_{\text{Telescope}}\rvert < 2\,\text{mrad}$ |

time shift and the z residuals were calculated with respect to the fitted TPC track. In the xy plane the residuals of TPC hits with respect to the telescope track were used to extract the single electron resolution in xy. For the resolution studies runs at three different z stage positions of the TPC were selected where the beam gave hits in the central chips. The data of 14 central chips (9, 12, 21, 21, 20, 17, 16, 2, 3, 6, 7, 30, 21, 26 and 27) was used. Two chips (8 and 13) were left out because of the E field deformations caused by the short circuit in chip 11.

The track selections are summarized in table 2.

## 5. Results

### *5.1. Number of hits*

The distribution of the number of TPC track hits per chip - without requiring a matched Telescope track - are shown in figure 5 for the data without magnetic field and for the B = 1 Tesla data.

The mean number of hits is measured to be 124 and 89 in the B=0 and 1 Tesla data sets. The most probable values are respectively 87 and 64. Note that the B=0 data has a much larger Landau-like tail than the 1 Tesla data. Also the fluctuations in the core of the distribution are larger. The mean time over threshold for the B=0 T is 0.68 µs and 0.86 µs at a 1 Tesla field. This means that the deposited charge per hit is smaller for the 0 T data. The most probable value for the total deposited charge is similar for both data sets. These

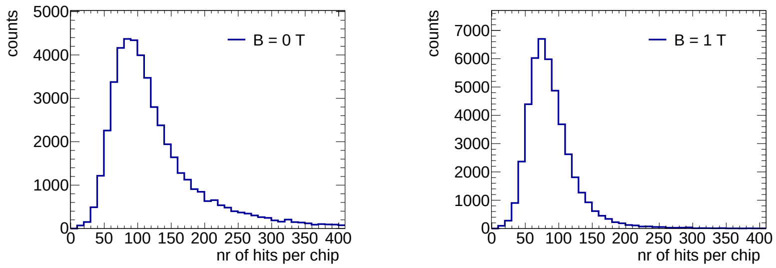


Figure 5: Distribution of the number of hits per per chip for B=0 (left) B=1 Tesla data.

numbers are in agreement with the predictions of [14] 106 electron-ion pairs for an 6 $GeV/c$ electron at B=0 , crossing 236 pixels or 12.98 mm and a detector running at 85% single electron efficiency.

### *5.2. Hit resolution in the pixel plane*

The resolution of the hits in the transverse plane ($xy$) was measured as a function of the predicted drift position ($z$). Only hits are used crossing the fiducial region defined by central core of the beam and staying 20 pixels away from the chip edges. The resolution for the detection of ionisation electrons $\sigma_x$ is given by:

$$\sigma_x^2 = \frac{d_{\text{pixel}}^2}{12} + d_{\text{track}}^2 + D_T^2(z - z_0), \tag{2}$$

where $d_{\text{pixel}}$ is the pixel pitch size, $d_{\text{track}}$ the uncertainty from the track prediction, $z_0$ is the position of the grid, and $D_T$ is the transverse diffusion coefficient. The resolution at zero drift distance $d_{\text{pixel}}/\sqrt{12}$ was fixed to 15.9 µm and $d_{\text{track}}$ to 30 µm for B=0 and 42 µm for B = 1 Tesla data.

The expression (2) - leaving $z_0$ and the $D_T$ as free parameters - is fitted to the B=0 T data shown in Figure 6. The fit gives a transverse diffusion coefficient $D_T$ of 287 µm/$\sqrt{cm}$ with negligible statistical uncertainty. The measured value is in agreement with value of $287 \pm 4$ µm/$\sqrt{cm}$ predicted by the gas simulation software Magboltz [15]. The values of the diffusion coefficients depend on the humidity that was not precisely measured during the testbeam. The humidity strongly affects the drift velocity. Therefore the drift velocity prediction from

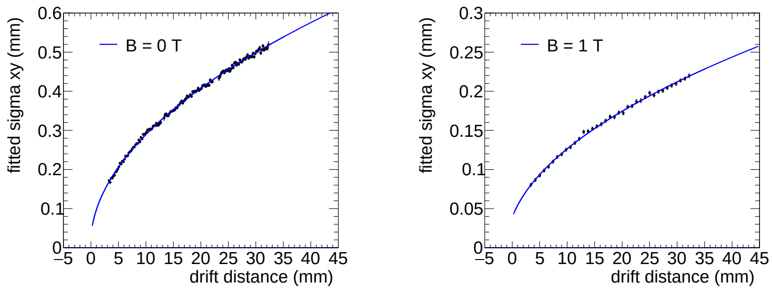


Figure 6: Resolution in the pixel plane (back points) using the resolution function given in equation (2) (blue line).

Magboltz was used to determine the water content per run and predictions for the diffusion coefficients could be obtained.

A fit to the B=1 T data shown in Figure 6 gives a transverse diffusion coefficient $D_T$ of $120\,\mu\text{m}/\sqrt{cm}$ with negligible statistical uncertainty. The measured value is in agreement with the value of $119 \pm 2\ \mu\text{m}/\sqrt{cm}$ predicted by Magboltz.

### *5.3. Hit resolution in the drift direction*

The resolution for the detection of ionisation electrons $\sigma_z$ is given by:

$$\sigma_z^2 = \sigma_{z0}^2 + d_{\text{track}}^2 + D_L^2(z - z_0), \tag{3}$$

where $\sigma_{z0}$ is the resolution at zero drift distance, $d_{\text{track}}$ the expected track uncertainty and $D_L$ the longitudinal diffusion constant. Only track crossing the fiducial region were accepted and hits with a ToT value above $0.6\,\mu\text{s}$ were selected. Because of the time jitter, the fitted TPC track is used for the drift residuals. For the z drift distance the Telescope prediction at the hit was used. The expected uncertainty on the track is $25\,\mu\text{m}$ at z = 0 mm and $75\,\mu\text{m}$ at z = 30 mm.

The expression (3) - leaving $\sigma_{z0}$ and the $D_L$ as free parameters - is fitted to the B=0 T data shown in Figure 7. The value of $z_0$ was fixed to the result of the fit in the xy plane. The value of $\sigma_{z0}$ was measured to be $138\,\mu\text{m}$. The longitudinal diffusion coefficient $D_L$ was determined to be $265 \pm 1\ \mu\text{m}/\sqrt{cm}$,

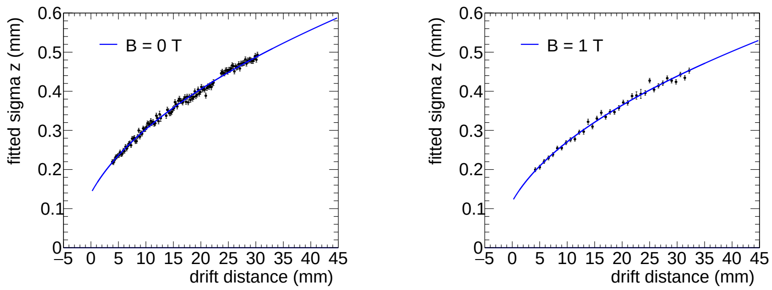


Figure 7: Resolution in the drift plane for hits with a ToT above 0.60 µs. The data are fitted with the expression of equation (3).

which is higher than the expected value $236 \pm 3$ µm/$\sqrt{cm}$ from a Magboltz calculation [15].

A fit to the B=1 T data shown in Figure 7 gives a longitudinal diffusion coefficient $D_L$ of $250 \pm 2$ µm/$\sqrt{cm}$. The measured value is in agreement with the value of $245 \pm 4$ µm/$\sqrt{cm}$ predicted by Magboltz. The fitted value of $\sigma_{z0}$ was 133 µm.

A selected TPC track in the B=0 T data has on average 1000 hits. The tracking precision in the middle of the TPC was derived on a track by track and found to be on average 9 µm in the precision plane and 13 µm in z. The angular resolution in dx/dy was on average 0.19 mrad and for dz/dy 0.25 mrad. It is clear that the position resolution in the TPC in the precision and drift coordinates is impressive for a tracklength of (only) 158 mm. The values are smaller than the uncertainty on the track prediction from the silicon telescope of 26 µm on average that is dominated by multiple scattering.

## 6. Conclusion and outlook

A Time Projection Chamber module with 32 GridPix chips was constructed and the performance was measured using data taken in a test beam at DESY in 2021. The analysed data were taken at electron beam momenta of 5 and 6 $GeV/c$ and at magnetic fields of 0 and 1 Tesla(T).

The result for the transverse diffusion coefficient $D_T$ is 287 µm/$\sqrt{cm}$ at B = 0 T and $D_T$ is 120 µm/$\sqrt{cm}$ at B = 1 T. The longitudinal diffusion coefficient $D_L$ is measured to be 268 µm/$\sqrt{cm}$ at B = 0 T and 250 µm/$\sqrt{cm}$ at B = 1 T. Results for the tracking systematical uncertainties in xy were measured to be smaller than 14 µm with and without magnetic field. The tracking systematical uncertainties in z were smaller than 14 µm (B = 0 T) and 22 µm (B = 1 T).


## Acknowledgements

The 32 Gridpix module could not be constructed without the enormous effort and creative energy that Fred Hartjes has invested in it over several years. This research was funded by the Netherlands Organisation for Scientific Research NWO. The authors want to thank the support of the mechanical and electronics departments at Nikhef and the detector laboratory in Bonn. The measurements leading to these results have been performed at the Test Beam Facility at DESY Hamburg (Germany), a member of the Helmholtz Association (HGF).


## References


[1] C. Ligtenberg, et al., Performance of a GridPix detector based on the Timepix3 chip, Nucl. Instrum. Meth. A 908 (2018) 18–23. arXiv:1808.04565, doi:10.1016/j.nima.2018.08.012.

[2] C. Ligtenberg, et al., Performance of the GridPix detector quad, Nucl. Instrum. Meth. A 956 (2020) 163331. arXiv:2001.01540, doi:10.1016/j.nima.2019.163331.

[3] J. Kaminski, Y. Bilevych, K. Desch, C. Krieger, M. Lupberger, GridPix detectors - introduction and applications, Nucl. Instrum. Meth. A845 (2017) 233–235. doi:10.1016/j.nima.2016.05.134.

[4] C. Ligtenberg, A GridPix TPC readout for the ILD experiment at the future International Linear Collider, Ph.D. thesis, University of Amsterdam

(2021).
URL https://www.nikhef.nl/pub/services/biblio/theses_pdf/thesis_C_Ligtenberg

[5] M. Lupberger, Y. Bilevych, H. Blank, D. Danilov, K. Desch, A. Hamann, J. Kaminski, W. Ockenfels, J. Tomtschak, S. Zigann-Wack, Toward the Pixel-TPC: Construction and Operation of a Large Area GridPix Detector, IEEE Trans. Nucl. Sci. 64 (5) (2017) 1159–1167. doi:10.1109/TNS.2017.2689244.

[6] T. Poikela, J. Plosila, T. Westerlund, M. Campbell, M. De Gaspari, X. Llopart, V. Gromov, R. Kluit, M. van Beuzekom, F. Zappon, V. Zivkovic, C. Brezina, K. Desch, Y. Fu, A. Kruth, Timepix3: a 65K channel hybrid pixel readout chip with simultaneous ToA/ToT and sparse readout, JINST 9 (05) (2014) C05013.

[7] J. Visser, M. van Beuzekom, H. Boterenbrood, B. van der Heijden, J. I. Muñoz, S. Kulis, B. Munneke, F. Schreuder, SPIDR: a read-out system for Medipix3 & Timepix3, Journal of Instrumentation 10 (12) (2015) C12028. doi:10.1088/1748-0221/10/12/C12028.

[8] B. van der Heijden, J. Visser, M. van Beuzekom, H. Boterenbrood, S. Kulis, B. Munneke, F. Schreuder, SPIDR, a general-purpose readout system for pixel ASICs, JINST 12 (02) (2017) C02040. doi:10.1088/1748-0221/12/02/C02040.

[9] F. Hartjes, A diffraction limited nitrogen laser for detector calibration in high energy physics, Ph.D. thesis, University of Amsterdam (1990).
URL https://www.nikhef.nl/pub/services/biblio/theses_pdf/thesis_F_Hartjes.pdf

[10] J. D.-E. e. a. R. Diener, The desy ii test beam facility', Nuclear Instruments and Methods in Physics Research. Section A: Accelerators, Spectrometers, Detectors and Associated Equipment 922 (2019) 265–286. arXiv:1807.09328, doi:10.1016/j.nima.2018.11.133.

[11] D. Cussans, Description of the JRA1 Trigger Logic Unit (TLU), v0.2c, EUDET Collaboration (2009).
URL https://www.eudet.org/e26/e28/e42441/e57298/EUDET-MEMO-2009-04.pdf

[12] J. Kröger, S. Spannagel, M. Williams, User manual for the corryvreckan test beam data reconstruction framework, version 1.0 (2019). arXiv:1912.00856.

[13] C. Kleinwort, General broken lines as advanced track fitting method, Nuclear Instruments and Methods in Physics Research Section A: Accelerators, Spectrometers, Detectors and Associated Equipment 673 (2012) 107–110. doi:10.1016/j.nima.2012.01.024.

[14] R. Veenhof, Garfield - simulation of gaseous detectors, version 9, Reference W5050 (1984-2010).
URL https://garfield.web.cern.ch

[15] S. F. Biagi, Monte Carlo simulation of electron drift and diffusion in counting gases under the influence of electric and magnetic fields, Nucl. Instrum. Meth. A421 (1-2) (1999) 234–240. doi:10.1016/S0168-9002(98)01233-9.